Colloid Polym Sci 273:202–218 (1995)

LEADING CONTRIBUTION

G. Schön
U. Simon

A fascinating new field in colloid science: small ligand-stabilized metal clusters and their possible application in microelectronics

Part II: Future directions

Received: 7 July 1994
Accepted: 10 August 1994

Prof. Dr. G. Schön (✉) · U. Simon
Institut für Anorganische Chemie
Universität Essen
Schützenbahn 70
45127 Essen, FRG

Abstract Small metal clusters, like $Au_{55}(PPh_3)_{12}Cl_6$, which fall in the size regime of 1 – 2 nm are colloidal nanoparticles with quantum properties in the transitional range between metals and semiconductors. These chemically tailored quantum dots show by the Quantum Size Effect (QSE) a level splitting between 20 and 100 meV, increasing from small particle sizes to the molecular state. The organic ligand shell surrounding the cluster acts like a dielectric "spacer" generating capacitances between neighboring clusters down to 10^{-18} F. Therefore, charging effects superposed by level spacing effects can be observed. The ligand-stabilized colloidal quantum dots in condensed state can be described as a novel kind of artificial solid with extremely narrow mini or hopping bands depending on the chemically adjustable thickness of the ligand shell and its properties. Since its discovery, the Single Electron Tunneling (SET) effect has been recognized to be the fundamental concept for ultimate miniaturization in microelectronics. The controlled transport of charge carriers in arrangements of ligand-stabilized clusters has been observed already at room temperature through Impedance Spectroscopy (IS) and Scanning Tunneling Spectroscopy (STS). This reveals future directions with new concepts for the realization of simple devices for Single Electron Logic (SEL).

Part II presents models and connections between microscopic and macroscopic level, regardless of whether there already exist suitable nanoscale metal cluster compounds, and is aimed at the ultimate properties for a possible application in microelectronics.

Key words Ligand-stabilized metal clusters – nanoparticles – quantum dots – single electron logic – microelectronic devices

Quantum properties of ligand-stabilized metal cluster systems

In part I [1], we briefly reported the various investigations concerning ligand-stabilized metal clusters and their physical properties, as known up to now. Furthermore, we discussed in greater detail, but by no means comprehensively, some partially unexplained experimental findings in reference to electronic, electrical and some optical properties. Here, and in the following section, we address connections between the microscopic and macroscopic level, including experimental findings and, in greater scope, tentative theories and speculative models. In the final sections, we dare to develop the ultimate properties and the potential of these cluster structures as future directions in metal cluster science, together with a scenario of pos-

sible applications in microelectronics. In doing so we hope to *stimulate preparative chemists, nanoscale-scientists and theorists to embark on some joint efforts towards ultimate miniaturization with electrons.*

Besides the "Bohr–Sommerfeld Atom Model," none of the presently existing microcluster models is easily applicable for chemists. The cluster status is usually approached either from the aspect of the Molecular Orbital (MO) theory, describing the cluster as some kind of large molecule, or from the aspect of a solid, presuming a band structure. Shell or Jellium [2] models proceed from symmetric bodies with more or less delocalized electrons which can be embedded in dielectrics having potentials corresponding to the "Woods-Saxon-Potential" [3, 4]. However, due to a substantial lack of experimental data concerning metal clusters in the 1 – 2 nanometer region – i.e., in the environment of the *Quantum Size Effect* (*QSE*) – the improvement of existing model approaches is very time consuming.

Based on simple physical, as well as on chemical and solid-state chemistry principles, we will present in this section an "ab initio" set of very simple *quantum properties* for metal particles a) *isolated and* b) *condensed in collective interaction.* This will provide a helpful point of orientation in evaluating or predicting the real macroscopic and microscopic properties of these systems.

a) *Isolated metal clusters* (and dispersions or dilutions with inter-particle distances >2 nm) in polar or non-polar matrices:

– Metal clusters with diameters up to 2 nm are natural so-called Q-particles or quantum dots. They accommodate, independent of the remaining structure of electronic states, a certain quantity of "conducting electrons". These electrons "feel" the confinement due to the low dimension and behave like "particles in the box" with discrete energy states. Figure 1 illustrates, using the two-shell Au_{55} cluster as an example, three different possibilities for the extension of the box: the inner core of the cluster, the surface of the metal core, and the complete cluster including the ligand shell.

– On the frontier between insulator and metal or semiconductor, the most simple and vivid model cases involve one

Fig. 1 "Metallic" quantum confinement within $Au_{55}(PPh_3)_{12}Cl_6$, the "normal" Au_{55} (c.f. Fig. 1, part I). This cluster type offers three potential geometric possibilities for electron localization

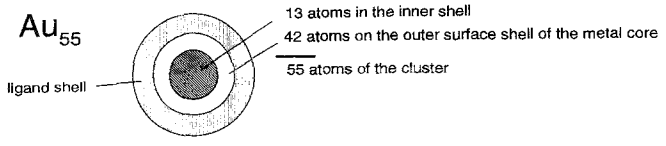

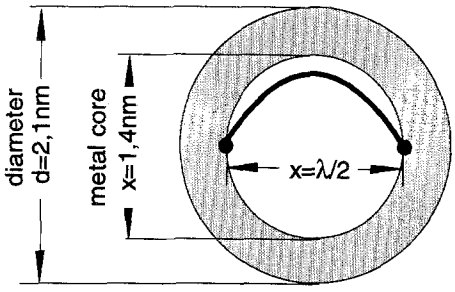

Fig. 2 "Conducting electron" in the ground state, localized in the metal core of Au_{55}

or two conducting electrons in their ground state with $x = \lambda/2$ (λ = de Broglie wavelength, compare Fig. 11, section 6.1, part I) confined in the metal core of a cluster. Figure 2 illustrates this situation for a one-dimensional planar wave, again using the size of the normal Au_{55} cluster.

Similar to Bohr's model of the hydrogen atom with the first *K*-shell, we would like to speak of *s* electrons in a "cluster"-σ-orbital*). This concept would mean that wave functions of such electrons should exist, which are in turn tailored by the size and shape of the cluster [5, 6].

Note. This conception is not based on new ideas, even though, in trying to understand the structure of matter, it has become customary during the 50 years after Bohr to work only with molecular orbitals and bands, each consisting of atom orbitals or molecule orbitals. Furthermore, *regarding matter composed of collectives like clusters, their bonding has not been regarded in terms of other wave functions of "binding" electrons.* The consideration of such wave functions only started in the last few years in the field of microelectronics, but here still only with respect to semiconductors, not with small metal particles. The technological trend of applying 1–2 nm clusters as natural *Q*-particles to solve the problem of miniaturization as well as the availability of such clusters in mol-scales requires a change in this view.

b) *Condensed clusters* (collectives of more than one cluster in densest packing, i.e., multiple quantum wells with an inter-particle distance < 2 nm), as pairs, chains or layers of ligand-stabilized clusters (c.f. sections 3.1 and 3.2) or as sections of ordered cluster arrangements embedded into non-conducting media (corresponding to the ligand shells) or host lattices:

– Among these numerous possibilities, such "defined" cases (regular structures) are assumed when the ligand

*) This orbitals are not equivalent with the orbitals of shell models for clusters [7].

Colloid & Polymer Science, Vol. 273, No. 3 (1995)

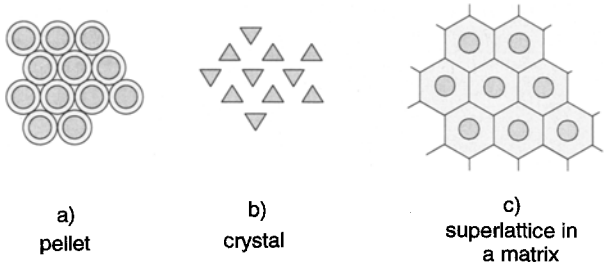

Fig. 3a–c Examples for multiple quantum well cluster-collectives: a) Metal clusters condensed in an artificial pellet, b) "triangular" quantum dots (c.f. fig. 8, part I) in a crystal and c) in a matrix or supperlattice like zeolites

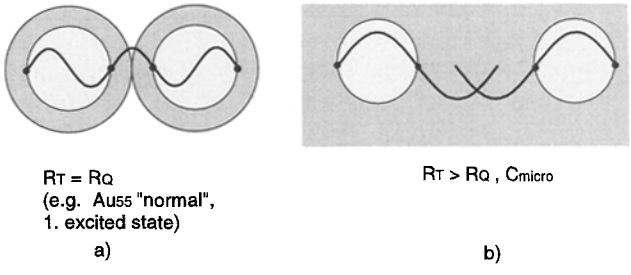

Fig. 4a–b Chemical size-tailoring of ligand shells and intercluster spacing; varying the tunnel resitance R_T and capacitance C_{micro} or the conditions necessary for coupling of wave functions

shells (0.3–1 nm thick) are in direct contact with each other (Fig. 3a) or when conducting clusters are crystallized or embedded into a matrix (Fig. 3b–c) so that a suitable tunnel or hopping distance exists for electrons. In such structures a microscopic capacitance C_{micro} is maintained between the clusters via the ligand shells or the insulating sections of the crystals and host matrix. "Inside" the metal core of the cluster the quantum resistance R_Q is attributed to the conducting electrons. Normally, the tunnel resistance R_T between the clusters will be larger than R_Q.

– The values for C_{micro} and R_T in such "multiple quantum-well" structures depend on the relationship between the size of the metal core and the thickness of the ligand shell (c.f. Table 2 for Au_{55}, section 6.1, part I) and hence the distance of the metal cores as well as the chemical nature of the cluster. Fundamentally, one can think about a number of different possibilities (Fig. 4a–b) like, for example, unhindered coupling of electron waves (wave propagation) with $R_T = R_Q$ or tailored values of R_T and C_{micro}. Taking advantage of these various combinations, a new field of coupled, collective properties is opened which is also of special interest for basic research in theoretical physics.

Connections between the microscopic and macroscopic level, tentative explanations and models

The evaluation of the system properties employing the above described "set" of microscopic properties for ligand-stabilized clusters should begin with the interpretation of the impedance measurements and the explanation of the optical properties displayed by macroscopic condensed cluster samples having approximately closest sphere packing.

Electronic pecularities of condensed cluster samples

Up to now, the most striking feature observed for all condensed cluster samples investigated by *Impedance Spectroscopy* (*IS*) is the appearance of *Debye-type low-frequency relaxations* with characteristic relaxation times τ_{macro} in the kHz range up to the MHz range. Cole–Cole type relaxations are also seen showing no linear dependence of the sample's macroscopic geometry. From the capacitance C_D of the Debye process, microscopic capacitances between clusters can be determined which are in accordance with *Scanning Tunnel Spectroscopy* (*STS*) measurements (c.f. section 6.1, part I and section 2.3). The importance of C_{micro} for SET processes at room temperature and for SEL with metallic quantum dots has been recognized very early [8–10]. It should be emphasized that if the samples were unordered heterogeneous solids, the appearance of just a single Cole–Cole relaxation would be nothing new (as mentioned in section 6.1, part I). However, for the ligand-stabilized clusters, the presence of partially well-ordered, densest packed quantum dots has been established by STM measurements like in Fig. 5. This image shows the surface topography of a densest packed cluster sample [11].

Two distinguishable size distributions can be detected. One starts with the most frequent size of 2.1 nm, which agrees with the diameter of a single cluster including its ligand shell as established by various techniques [12, 13, 46]. The second gives an average diameter of approximately 4.3 nm, which corresponds to an octahedral arrangement of exactly six Au_{55} clusters. Beside these two groups, only a few larger particles can be seen. For STM-investigations and impedance measurements, samples filtered on Anotope® (pore-width 20 nm) were used because the freshly prepared clusters tend to aggregate into "superclusters," consisting mainly of 13 or 55 Au_{55} clusters in a geometrical magic arrangement. Thirteen-membered superclusters with a diameter of 6 nm have been discovered to be building blocks of natural "quantum wires" prepared along a linear displacement of a crystalline substrate [14] or graphite [15]. Using the method of Debye

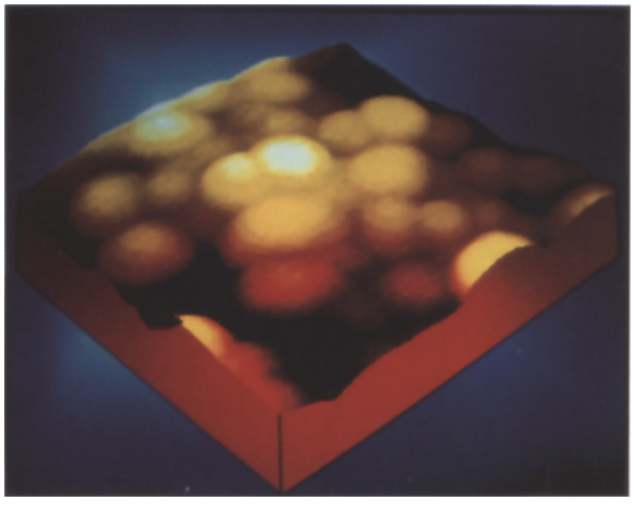

Fig. 5 A Scanning Tunnel Microscope (STM) image illustrating the dense packing in the compressed discs and the spherical habitus of the "normal" Au_{55} clusters each with a diameter of 2.1 nm (c.f. Fig. 2, part I)

function analysis for x-ray diffraction measurements [16] aggregates of 55 Au_{55}-clusters have also been detected as well as a small quantity of larger particles like Au_{147} and Au_{309} ($\approx$4 mol%). Also, an icosahedral structure of the constituent Au_{55}-building-units is indicated instead of a cuboctahedral arrangement (c.f. Fig. 1a, part I) as supposed from the results of Mössbauer [17] and EXAFS [18, 19] measurements. The general tendency towards self organization has also been observed during the electrochemical synthesis of naked Au_{13}-clusters via decomposition of $Au_{55}(PPh_3)_{12}Cl_6$. The naked Au_{13}-clusters stabilized themselves through aggregation to larger clusters with preferring geometrically magic numbers like $(Au_{13})_{13}$ or $((Au_{13})_{13})_{13}$ and so on [12].

These observations are important with respect to applications in multijunction quantum devices in the microelectronics, as suggested in section 3. On the one hand, these results support the model for the impedance spectroscopy on condensed cluster arrangements. On the other hand, they imply the possibility that single clusters can be handled and structured to give well-defined (e.g. in one-, two- or three-dimensional) arrangements. The latter is of enormous interest and thus appears to be a new task for colloid chemistry.

These findings on condensed ligand-stabilized clusters have also been confirmed by impedance measurements on crystallized $Cu_{70}Se_{35}(PR_3)_{22}$ and $Cu_{146}Se_{73}(PR_3)_{30}$ quantum dots. Here, the clusters form regularly arranged metallic conducting islands (c.f. Fig. 3 and Fig. 8, part I) in which a microscopic capacitance C_{micro} is built up across the ligand shells between the metallic clusters, leading to the same dielectric response: depending on the crystal quality, besides the pronounced Debye relaxation domain a Cole–Cole relaxation can also be found [20].

Brick layer and easy path model

For cermets and other two-phase heterogeneous microstructures, the impedance spectroscopic "*brick layer model*" [21, 22], a closest packed array of cubic shaped grains separated by flat grain boundaries, has proved to be a successful approximation. The STM images indicate that in condensed samples of ligand-stabilized Q-particles zones of perfect packing (bulk or grain interior phase g_i) with a thickness D exist as well as small zones with irregular, disturbed sphere packing (grain boundary phase g_b). The "grain boundary" of thickness d in perfect, compressed discs often seems to consist of either one single disturbed cluster, a cluster pair or one larger cluster. According to this, the picture of the "ideal imperfect crystal" with narrow grain boundaries should be valid for crystalline cluster arrangements (Fig. 6).

The current flow is assumed to be one dimensional and its curvature is neglected. Since two relaxation regions are always observed, according to the model the conduction along the grain boundaries is negligible while the conduction through the grains and across grain boundaries dominates. It is evident that this assumption is compatible with our previous circuit equivalent having the microscopic relationship for the conductivities $\sigma_{gi} > \sigma_{gb}$ (c.f. Fig. 10a–d, section 6.1 part I). Despite this condition, it is found in many instances that the activation enthalpies for the two conduction processes are equal or very similar. This can be explained by the "*easy path model*" [23, 24].

The separation of the microscopic single current paths is shown in Fig. 7a–b. The resulting macroscopic conduc-

Fig. 6 Brick layer model of an ideal grain (grain interior phase gi) with a grain boundary phase (gb) of condensed cluster material

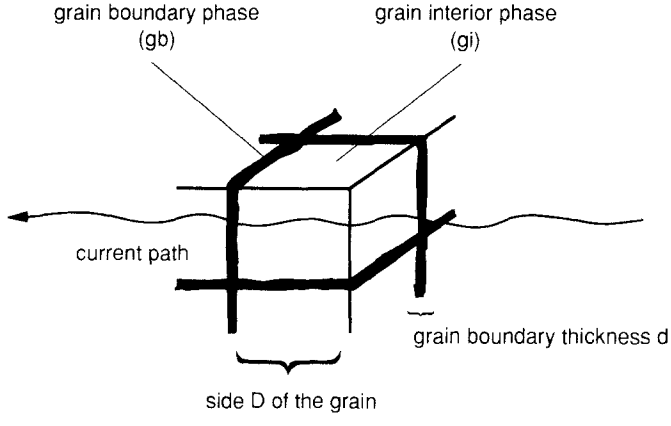

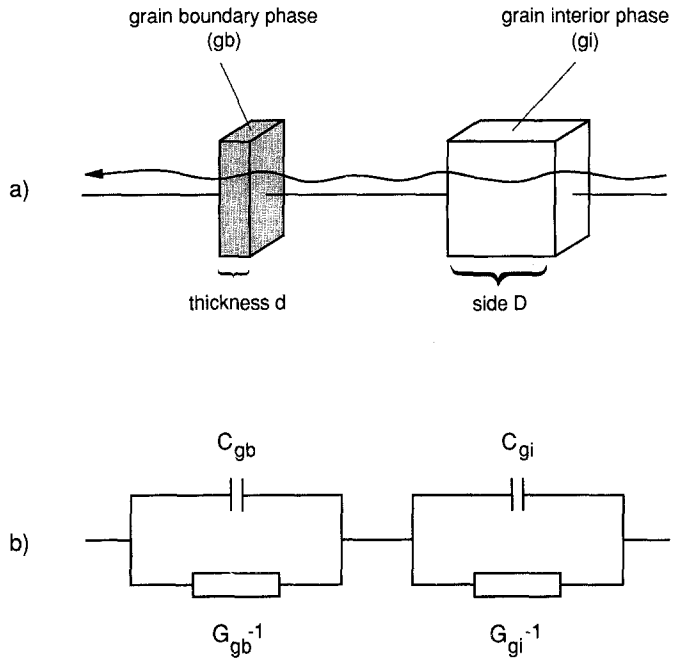

Fig. 7a–b a) Separation of the microscopic "current paths" in the brick layer model and b) the circuit equivalent for grain boundary and grain interior

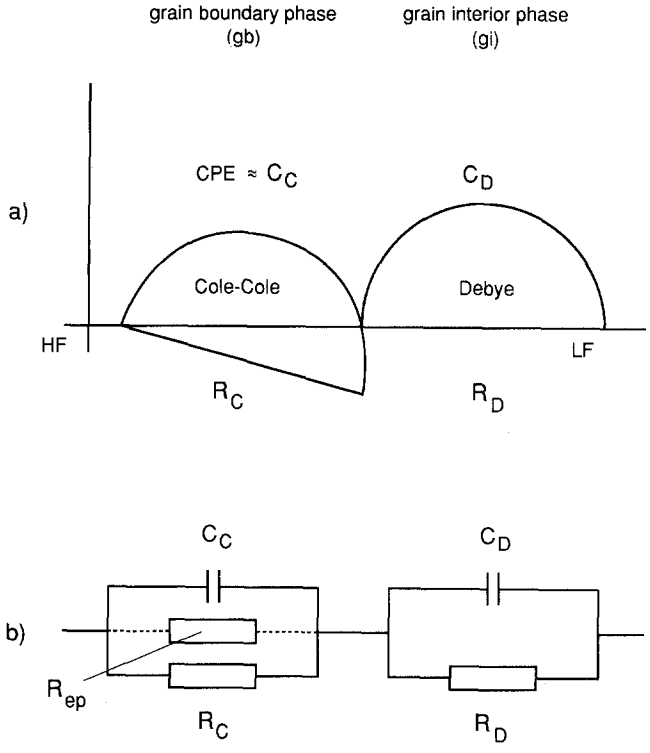

Fig. 8a–b The model given in Fig. 7 transformed to the experimental situation: a) Expected resoluted impedance spectrum in the complex plane and b) real circuit equivalent

tivities G_{gb} and G_{gi} are caused by grain boundaries and grain interior (bulk). Accordingly, C_{gb} and C_{gi} are the microscopic capacitances of the sample. For $d < D$ the immitance equations for a macroscopic system consists of two parts, a conductive and a capacitative,

$$G_{gi} = \sigma_{gi} \qquad Cgi = \varepsilon_{gi}$$
$$G_{gb} = 3\sigma_{gb}/x_{gb} \qquad C_{gb} = 3\varepsilon_{gb}/x_{gb} \tag{1}$$

conductive part capacitive part

where x_{gb} is the respective volume fraction, and ε_{gi} and ε_{gb} are the permittivities.

Applying these equations to the experimentally measured quantities, the appropriate expected and real spectra are given in Fig. 8a and b, respectively (compare with the spectrum of the densest packed normal Au_{55} given in Fig. 10a, section 6.1 of part I).

Then the following equations result:

$$G_D = R_D^{-1} = \sigma_{gi} \qquad C_D = \varepsilon_D$$
$$G_C = R_C^{-1} = 3\sigma_{gb}/xgb \qquad C_C = 3\varepsilon_C/x_{gb} \tag{2}$$

conductive part capacitive part

Often, one refers loosely to G_{gi} (or R_D^{-1}) and G_{gb} (or R_C^{-1}) as "grain interior" and "grain boundary" conductivities. But it must be kept in mind that they are usually corrected for the macroscopic shape of the sample, e.g., by the cell constant. Furthermore, it must be pointed out that G_{gb} can be greater than G_{gi} without implying the assumption $\sigma_{gb} > \sigma_{gi}$. Due to the differing shapes of the ideal grains and very different relationship between d and D, it is easy to understand why the frequency positions and the ratios of the two relaxation regions in the impedance spectra (Fig. 10a–d, section 6.1, part I) of the various cluster samples look so different from one another. From the simplified equations (2) it can be seen that in first approximation, C_D is directly related to the grain interior permittivity, and the resistivity R_D of the Debye relaxation for the normal Au_{55} cluster corresponds to the microscopic resistivity of the ideal grain. The latter means that based on the experimental data in the high temperature region the condition $R_T \approx R_Q$ is roughly valid which justifies the adjustment of the SIMIT-data [14, 25] (see Section 6.1 of part I). For more complicated spectra and clusters with less perfect packing or matrix-stabilized [26], it must be corrected to the proper volume fraction and distribution.

In Fig. 9a and b a complete description of the brick layer model in terms of the cluster samples is given. The microscopic enlargement in Fig. 21b makes the two processes visually comprehensive to a certain extent.

The experimental volume fractions x_{gb} estimated by Eqs. (2) in the high temperature region for the different

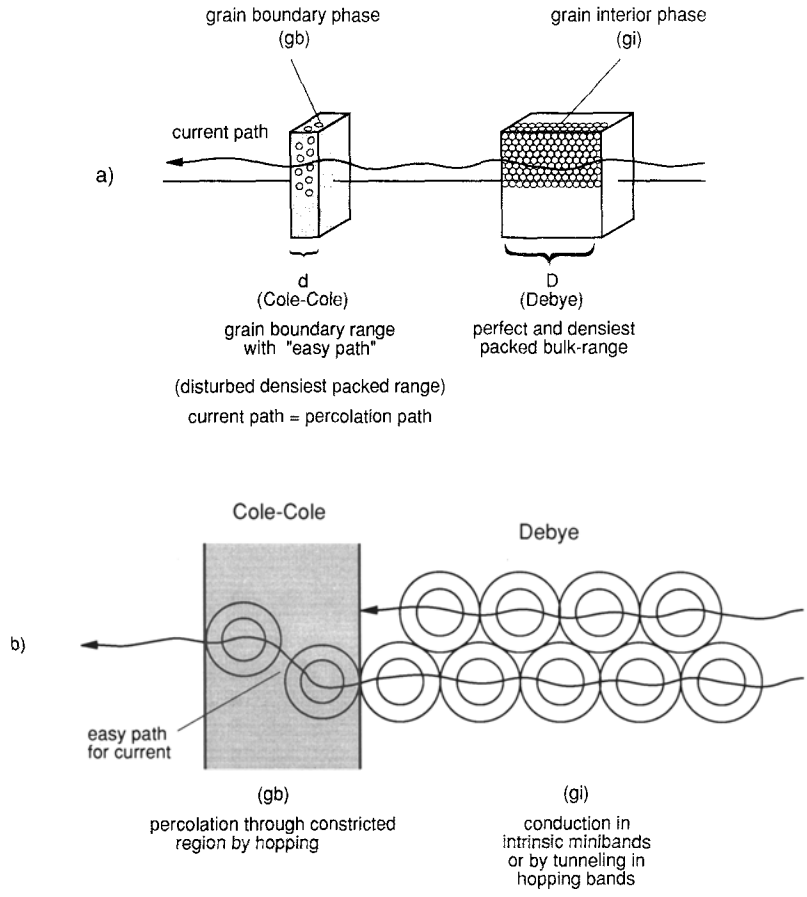

Fig. 9a–b a) Description of a condensed cluster material by a microscopic cermet model with grain boundary and interior phase. b) The adequate microscopic enlargement showing percolation through a constricted region by hopping and conduction in intrinsic minibands or by tunneling in hopping bands

Au_{55}-samples, yield an average grain size for a defined grain boundary thickness d. If the diameter of one cluster is set to d, "normal" Au_{55} undisturbed arrays between 10 and 100 clusters are then obtained.

Figure 9b clearly indicates that one of the assumptions of the brick layer model is no longer valid, namely, a continuous grain boundary region separating the individual grains. This conforms to the model of Bauerle [24], who suggested that for systems with $\sigma_{gi} > \sigma_{gb}$ – where the activation enthalpies for the two conductivities are often equal or very similar – regions of the grain boundary having good intergranular contact exist. These regions are called *easy paths*. The idea was that charge carriers (originally migrating oxygen ions) are sequentially partly blocked at grain interiors and grain boundaries. As can be seen in Fig. 9b, the presence of an easy path through constricted areas in the grain boundary region is evident, i.e., where the ligand shells are in direct or near contact securing the percolation through the sample. This model including easy paths requires only a slight correction of the Cole–Cole link in the circuit equivalent (c.f. Fig. 8b) via a parallel resistance R_{ep} which must be dependent on the strength of the electric field in accordance to the nonohmic behavior (see section 6.1, part I). In addition, it can be seen that, where no path is available for a hopping or tunneling electron, only relaxation within the grain will take place, which was already explained in Section 6.2, part I by a "miniband"-conduction.

Single Electron Tunneling (SET) at ambient temperatures with chemically size-tailored quantum dots

The brick layer model roughly compares the cluster samples with the heterogeneous structure of cermets. But one must keep in mind that in this model, the size of the ideal grains above the cluster size level. Hence, the standardized capacitance C_D of the Debye process approximates the capacitance of these bulk regions with perfect cluster packing. As already mentioned in section 6.1, part I and in section 2.1, C_D can be divided into the microscopic partial capacitances C_{micro} of single clusters: Assuming n clusters per meter and a low concentration of grain boundaries, for "normal" Au_{55} with $n \approx 5 \cdot 10^8$/m an experimental value of $C_{micro} \approx 3 \cdot 10^{-18}$ F is obtained for one total cluster island. The values for C_{micro} for the different Au_{55}-variants as determined from other IS measurements (depending on the density of packing) range from 1 to $5 \cdot 10^{-18}$ F. Thus

Colloid & Polymer Science, Vol. 273, No. 3 (1995)

with respect to the second principal condition for *Single Electron Tunneling* (*SET*) (see section 3, part I) IS is a very easy way to estimate whether this effect is possible or not for clusters at ambient temperature [8, 10, 14].

The values listed above are in good agreement with tunnel capacitances determined from STM for the surface clusters of compressed Au_{55}-discs [15] and single clusters on a conducting substrate [27, 28]. Furthermore, the capacitances correspond with the calculations for a single cluster by a macroscopic electrostatic approach which amounts $C_{micro} \approx 10^{-18}$ F for a ligand dielectric constant of ≈ 4 [29]. But this is only a rough estimate with respect to the much more complicated situation in *Energy Quantized Single Electron Tunneling* (*OSET*) (see section 3, part I).

An exceptionally important aspect for microelectronics is the potential to construct from chemically synthesized quantum dots, SE-circuits which function at room temperature. For instance, the charging energy E_c with a capacitance $C_{micro} \approx 10^{-18}$ F for each of the four Au_{55}-variants would surmount the thermal energy k_BT by more than a factor 6, allowing the establishment of a Coulomb barrier. This will be most likely proven by the not yet completely evaluated STS-experiments [15] on compressed disks of $Au_{55}(PPh_3)_{12}Cl_6$, the "normal" Au_{55}, [30] at *ambient temperature* cited in part I. Current-voltage characteristics (I-U-curves, Fig. 10) show a distinct dependence of the tunnel-resistance as verified through the application of different distances between tip and sample. The curves also revealed the expected nonlinear behavior with the appearance of a blockade region up to 0.9 V.

Well reproducible fine structures in the differential conductivity (Fig. 11) having distances of about 100 mV will hopefully give hints on Coulomb- and quantum-size-effects. Especially interesting is information concerning the level splitting around the Fermi level of isolated Au_{55} quantum dots which were estimated independently in section 6, part I with approximately 100 meV. Since these structures are equivalent any for all surface clusters directed by the STM-tip, it may be assumed that the microprocess which causes the voltage offset occurs at the outer surface cluster(s). In comparison, the rest of the macroscopic sample, under the surface, seems to behave approximately like an ohmic resistor as proven by the course of the I-U-curve measured with a slight offset of approximately 100 mV in direct contact at the STS experiment. Since all the samples measured so far have rather high ohmic resistances, the results could also reflect the behavior of a "semiconductor". Alternatively, we are trying to obtain evidence for possible coupling mechanisms of the quantum dots in the Au_{55} solid (see section 6.2, part I).

With IS-measurements via macroscopic contacts, I-U-curves can also be obtained by extrapolating the dependence of the dc resistance of the sample from a superposed dc bias [10]. From these for Au_{55} an offset of about 20 V can be determined. Furthermore, an offset of 0.5 V has been reported, as seen through IS measurements, in the best case for Cu-chalcogenide cluster samples [20]. In our opinion, these results give hints on the presence of

Fig. 10 I-U-characteristics from Scanning Tunnel Spectroscopy (STS) on condensed "normal" Au_{55} at room temperature revealing most likely a Coulomb gap (c.f. Fig. 5, part I).

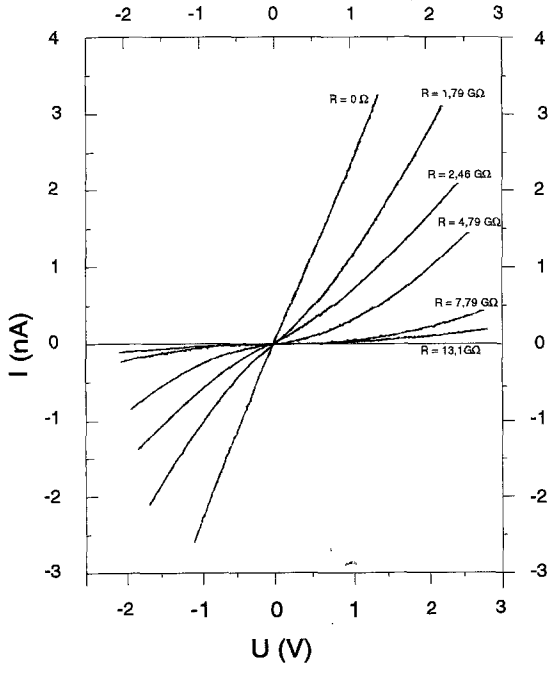

Fig. 11 The first but not yet completely evaluated fine structures observed in the differential conductivity of condensed "normal" Au_{55} clusters, as measured at room temperature, which point to Coulomb and quantum size effects

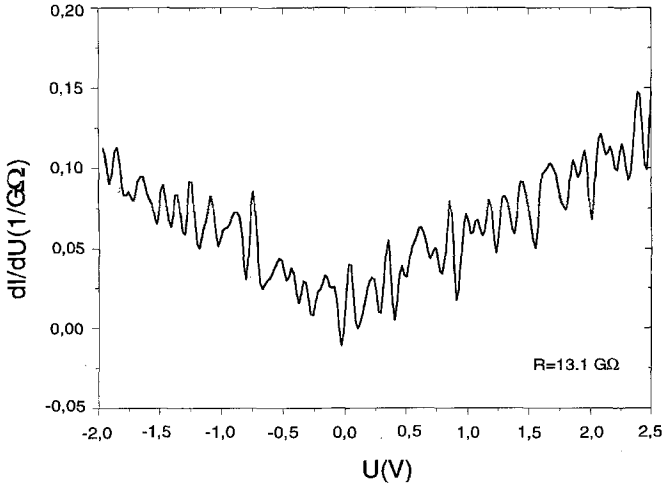

single electron current paths as predicted in ideal and closest packed cluster arrangements (parallel channels of macro-turnstiles see section 2.4, [17, 18, 24, 27]). In the ideal case, $|U| = e/C_{micro} = ne/C_D = Q/C_D$ is valid. Generally, serial defects are occurring at the grain boundaries (c.f. section 2.2) which are typically overcome by a field dependent "hopping"-process. For this reason the offset voltage may be higher or lower, but without giving any quantitative conclusion on the microscopic events.

The scenario described above indicates that ligand-stabilized quantum dots in closest packing or in crystals retain, in a certain way, their individuality. Any only because of this property could the investigation of their quantum properties *and* of the collective behavior on macroscopic samples be successful at all.

One is tempted to attribute the microscopic capacitance C_{micro} to a ligand shell- or crystalline environment capacitance. Since C_{micro} does not contribute to the conductivity [31], this suggests the presence of some type of classical dielectrics between the cluster cores [32]. Such a conclusion would correspond with the ordering of the measured activation enthalpies as $Au_{55} > Pt_{309} > Pd_{561}$ [33]. However, for this data no suitable geometrical criteria exist: In other words, the capacitance C_{micro} does not seem to be directly related to either the diameter of the cluster or the shortest distance between neighboring cluster cores. This is not surprising with respect to the case of QSET, considered in section 3 of part I, since the value of C_{micro} depends on the number of interacting electrons occupying the cluster. To further understand the problems in this field, it is necessary to invest a considerable amount of experimental and theoretical effort.

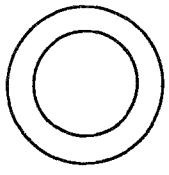

Meaning of the Debye low frequency relaxation regions and the connection to SET or rather QSET

Among other questions, an important problem remains of why the Debye relaxation frequencies can be observed for the bulk of undisturbed densiest packed or crystallized cluster arrangements in the LF region. Usually, electron resonances can only be detected in the microwave range at frequencies above 10^{10} Hz. To explain the Debye relaxation frequencies, a physical hypothesis which connects the macroscopic relaxation times τ_{macro} with microscopic characteristic times is needed. The Debye resonance for compact Au_{55} samples in the 10-kHz range seems to exemplify that a single electronic process, depending on its coupling to the environment, can be reached independently via different measurement method in completely different frequency ranges. This fact is already well-known and has been thoroughly analyzed for ionic relaxation processes in solid ion conductors [34]. Although it is possible to explain low frequency relaxations in cermets as polaron frequencies with the Einstein-relation for hopping conduction [35], in the following we will try to qualitatively explain the low frequencies by two, in fact, equivalent considerations. One is based on a *particle model as Single Electron Tunneling (SET)*, and the other on a simple *picture of propagating waves.*

The fundamental process for charge carrier transport in both the disturbed grain boundary region and the grain interior involves the transition of one electron between two neighboring clusters, a cluster pair. Chemically speaking, electrons in cluster pairs can no longer be considered as localized in one cluster. The cluster pair probably possesses a *common diluted electron gas* in extended states. But the appearence of Debye relaxation domains in the impedance spectra with a capacitive part proves that even in the high temperature range an intrinsic band conduction between the densest arranged clusters does not yet exist like in regular bulk semiconductors. Consequently, a microscopic tunnel barrier with a capacitance C_{micro} and a transition or tunnel resistance R_T is still present. But according to the measurements on Au_{55} this barrier is quite transparent and does not fulfil the condition $R_T \gg R_Q$, but rather $R_T > R_Q$ or $R_T \approx R_Q$. Since according to equations (2) (in section 2.2) applies for the standardized resistivity, $R_{D(macro)} \approx R_{Dmicro} \approx R_Q$.

As pointed out in section 3 of part I, the physics of *SET in systems of quantum dots* is more complicated because the standard macroscopic electrostatic approaches for C_{micro} and R_T fail and are only valid for in a rough description and approximation. Assuming $R_T \approx R_Q$ for condensed Au_{55} and $C_{micro} = 3 \cdot 10^{-18}$ F (see section 2.3), then from Eq. (1) (part I) a characteristic tunneling time τ_{micro} results

$$\tau_{micro} = R_T C_{micro} \approx R_Q C_{micro} \approx 10^{-13} \text{ sec} \approx \tau_{Dmicro}, \quad (3)$$

which may equal a local microscopic relaxation time τ_{Dmicro}. Consequently, both τ_{micro} and τ_{Dmicro} become as short as the characteristic time for the energy relaxation inside one cluster. This takes place with the transition of one electron to the next cluster, loading its capacitance C_{micro} and so on. In classical SET terms, this means that for an assumed corresponding *frequency* ν "SET" (as a limiting value for the electron propagation which would be in the same order of magnitude as the frequency of IR-VIS light) the capacitance C_{micro} will be loaded as fast as the

characteristic time for tunneling. Then, according to the SET relationship (2) (section 3 in part I) when $R_T \approx R_Q$ a current flow I_Q is obtained leading to the expression

$$\nu_{micro} = \nu_{Dmicro} \approx \nu_{\text{"SET"}} \approx eU/h, \quad (4)$$

which is formally related to the Bloch frequency for superconductivity in smallest dimensions for the tunneling of single Cooper pairs [36].

Relation (4) also defines, equally as well, for Au_{55} a microscopic relaxation time τ_{Dmicro} which gives an upper limit for an assumed microscopic "Debye frequency" ν_{Dmicro}. According to Eq. (2) and with Kirchhoff's laws for a *three-dimensional* closest arrangement of clusters $C_{D(macro)} = |n|C_{micro}$. Finally, there results

$$\tau_{Dmacro} = R_{D(macro)}C_{D(macro)} \approx R_{Dmicro}|n|C_{micro} = |n|\tau_{Dmicro} \quad (5)$$

Inserting $|n| \approx 10^8$ for Au_{55}, the macroscopic Debye frequency can be estimated $\nu_{Dmacro} \approx \nu_{Dmicro}/|n| \approx n_{\text{"SET"}}/|n|$ as measured in the 10–100 kHz region.

We arrive at the same result from the coupling of one-dimensional plane electron waves, say, in the first excited state like in Fig. 3a, section 1, or Fig. 12, section 2.5. The wave may propagate in the direction of the electric field along (or within) a cluster chain in a closest packed ideal sample. Then, in first approximation the following phase coupling law is valid:

$$\tau_{Dmacro} = |n|\tau_{Dmicro} \approx |n|R_TC_{micro} \quad (6)$$

where τ_{Dmacro} equals the operating time needed for the electron transport from electrode to electrode. In consideration of the ratio between the cluster diameter d (respectively the double ligand shell thickness) and the core diameter x, a macroscopic relaxation frequency of $\nu_{Dmacro} \approx 90$ kHz can be estimated.

It is known from lithographically-prepared, relatively short multiple quantum well chains (consisting of up to 40 links, but with $R_T \gg R_Q$), its SET transitions can in fact be synchronized with suitable ac frequencies to generate a "turnstile-effect" [37]. This means that the macrosystem behaves almost as if just as many QSET-transitions are proceeding as tunnel contacts during a definite phase of the macroscopic ac-resonance field. Solids consisting of densest packed ligand-stabilized metal clusters – like ideally packed compressed discs of the "normal" Au_{55} – or single crystals from such Q-particles should consequently behave like one single macroturnstile.

Potential models and the miniband structure of coupled Q-particles in a new kind of solids

To illustrate the elementary processes, suitable potential models for single electrons in natural quantum dots and their multiple quantum well structures (c.f. section 1, a) and b)) will be sketched. The simplest way to describe the electrons in a quantum dot is to apply the model of the Harmonic Oscillator; just one "cluster" σ-orbital (ground state) and the first excited state separated by the energy ΔE will be discussed. Based on the size of the normal Au_{55} cluster the energy of the ground state would be approximately 200 meV. Chemically speaking, ΔE is the difference of the HOMO level and the LUMO level, or for a band gap, the level spacing between the valence and conduction band. Here, both the picture of potential wells as it is applied in chemistry for activated processes, and that of electrons in a box-like potential are of practical use.

Figure 12 illustrates this for *a single cluster* based on the size of the normal Au_{55} cluster. Here, by chance the proportion of the core diameter and the double shell diameter has a "magic" relationship, 2:1. A geometrical picture arises, as if a planar wave can propagate unhindered through the barrier built up by the ligand shells between the clusters. This means that in the special case where $R_T = R_Q$ a so-called *"miniband"* [38] of a *"real" intrinsic semiconductor* with single delocalized electrons should be generated (c.f. section 6.2, part I). Such a total coupling of states, in which no capacitance C_{micro} acts between the clusters and where the clusters would lose their individuality, is not necessarily given in other types of

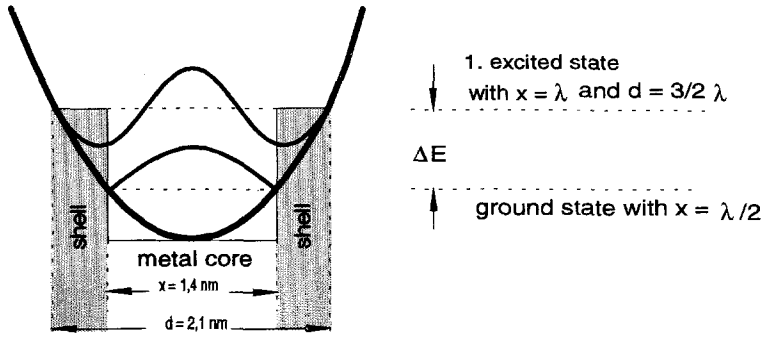

Fig. 12 Simplified potential well for the dimensions of "normal" Au_{55} according to Fig. 2 with a "cluster" σ-orbital and the first excited state for a single electron

cluster collectives or crystals of ligand-stabilized clusters. Depending on the dimension of the cluster and the ligand shell, a so-called *hopping semiconductor* [35] would result with other types of bands including the possibility of superlocalization [39]: here the hopping probability depends on the cluster size, the distance, and mainly on the quality of the packing (i.e., the periodicity of the arrangements of quantum dots). In this case the hopping resistance $R_H \approx R_T$ is larger than R_Q and the conductivity is thermally activated due to contributions by phonons from oscillations of the cluster itself in the collective [35] and, depending on the size of the cluster, due to the creation of charge carriers [40]. Between the clusters in the condensed state a capacitance C_{micro} is still maintained: for this type of condensation of new solids from ligand stabilized clusters an unexcelled manifold for chemically-tailored electron transitions arises between neighboring clusters by tunneling or hopping.

In Fig. 13 the situation is sketched for a *cluster pair* which may be directly located at a grain boundary, but, at the same time, be part of a well-defined arrangement of clusters (cluster I and cluster II, left part) and in which an electron transition has just occurred. Physically speaking, here a small polaron is created. An undisturbed region in the grain interior is adjacent to the cluster (to the right), where the above described mini bands can exist. When an electron becomes excited in cluster I, it can pass more or less immediately – depending on the conditions of localization – into the LUMO of cluster II and *at the same time into the miniband* (which is the conduction band of the collective). If this scenario happens inside the disordered grain boundaries, where the clusters distance is distributed, the further transport of charges can only be achieved by hopping.

In the following, we would like to use a chemical consideration [35]: After a transition of an electron the "cluster molecules" I and II differ due to the fact that one cluster has one exess electron and in the second cluster one electron is missing. Although only for a very short time, a local separation of charges has been established which can be described as *a disproportionation of the two initially identical "molecules" into different oxidation states.* The activation enthalpy for this disproportionation is the difference between the ionization energy and the electron affinity. For atoms this can be in the range of some eV, which is in the same order of magnitude as the state energies that participate. For ligand-stabilized metal clusters consisting of 55 atoms and with only 13 atoms forming the inner core, a level spacing of 100 meV was estimated (see Section 6, part I). According to this model, ΔE is in the same order of magnitude as the level spacing (which means that if *this* ΔE is measured, then alternatively Coulomb blockades or Coulomb energies or the band gap of the collective will be detected).

After excitation, the polaron-like state relaxes back to the ground state due to recombination of the electrons or holes. Or it propagates through the minibands of the densest packed cluster arrangements or crystals. This propagation continues – because the lifetime of small polarons is high due to weak interaction processes – until a disorder or a grain boundary blocks it. The amount of the total dc-conductivity is determined by the probability of percolation across the grain boundaries, which can only be passed by hopping.

Future directions in metal-cluster science and possible applications in Single Electronics (SE)

Currently, large industrial electronics companies are focusing on the lithographic-tailoring of quantum devices

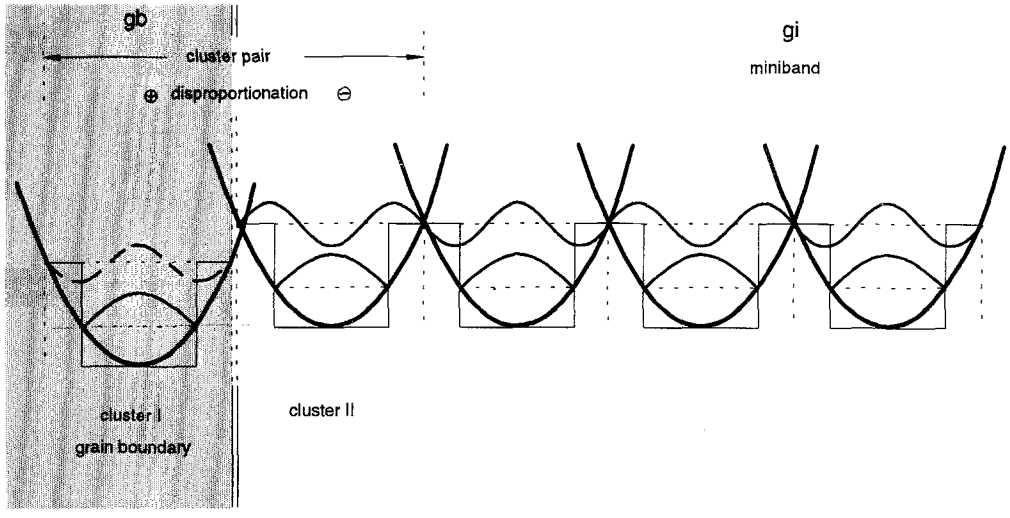

Fig. 13 Multiple potential wells for "normal" Au_{55} – with a disproportionated cluster pair at the grain boundary (gb) forming a miniband in the undisturbed grain interior (gi)

Colloid & Polymer Science, Vol. 273, No. 3 (1995)

[16] with "quantum dots" or "quantum wells" by surrounding mesoscopic semiconductor particles with a second material which has a larger band gap. This leads to a localization of electrons in these structures. However, due to technical difficulties of this method, which does not lead in every case to real quantum dots, other routes are also followed, namely, to synthesize "nano-crystals" in amorphous polymers and glasses or porous crystalline structures like zeolites [38]. In spite of all of these efforts, no breakthrough to generate absolutely identical quantum dots of approximately 1 nm in size has been achieved. Therefore, the industry is satisfied until the year 2010 to utilize the present technology to design structures down to 50 nm; besides well working switches today are still approximately 10 times larger. This means that already simple operations are associated with the motion of the huge amount of some millions of free electrons. However, presently due to the exploitation of charging, or more precisely of Coulomb effects, metallic circuits with tunnel junctions in submicrometer sizes are able to manipulate with individual charge carriers. This field is named *Single Electronics* (*SE*) (see section 3, part I).

Efforts employing physical techniques to diminish the size of metal particles to be used at room temperature as quantum devices with smallest capacitances C_{micro} still play only a marginal role in the big business of nanoelectronics. Even though *SET processes at room temperature* have already been observed in one- and two-dimensional systems:

The one-dimensional arrangement in a double-barrier tunnel junction has been realized by a STM-tip over Au droplets of approx 4 nm in diameter on a 1-nm-thick layer of ZrO_2 (tunnel barrier) on a flat Au substrate. The experimentally determined capacitance of the droplet-substrate junction is approximately $0.8 \cdot 10^{-18}$ F. The value is in good agreement with the theoretically estimated capacitance of approximately $1 \cdot 10^{-18}$ F based on the model of a parallel-plate capacitor with ZrO_2 as a defined dielectrics [41].

The two-dimensional tunnel junction array has been realized by using liquid crystal molecules (4'-n-heptyl-4-cyanobiphenyl) as tunnel junctions between deposited Pt and Pd droplets on a quartz substrate. The average size of the droplets is 1 nm and the average spacing is 0.2 nm to 0.5 nm. This arrangement has been contacted by a STM tip and a directly connected outer electrode. The I-U-characteristics of the arrays indicate a Coulomb blockade at approximately 100 mV at room temperature with an inter-droplet capacitance of $5 \cdot 10^{-18}$ F [42].

Only recently (due to the efforts in Essen as described in this paper) have suggestions for the application of *chemically tailored quantum dots in SET devices at room temperature* [8, 9, 14] been discussed with increasing weight. Meanwhile notable researchers and groups affirm the use of metal clusters which should bring about a trend to follow this strategy. We have demonstrated that ligand-stabilized metal and metal chalcogenide clusters are indeed chemically-tailored quantum dots, because they represent quantized matter with size-tailored wave functions for single conducting electrons.

The ligand shell as a potential barrier controls the single-electron transition between clusters. Therefore, a modification of the ligand shell allows the cluster capacitance C_{micro} to be tuned. It has also been shown that *novel solids consisting of size-tailored cluster collectives* which develop *mini bands or hopping bands* can be prepared by pressing or crystallizing ligand-stabilized metal clusters. As demonstrated in section 2.5, in these densest arrangements, the electronic states of neighboring clusters are connected to each other in such a way that in the ground states the electrons are localized in the clusters. The electrons are separated energetically from each other by the Coulomb energy for a single electron tunneling process. These unique properties of clusters and especially of clusters collectives make these materials very interesting for microelectronic devices based on SET.

The main emphasis for future applications in the SE should be focus on the utilization of SET processes in and at clusters, especially at room temperature. From low dimensional cluster arrangements one can progress to the collective behavior of novel kinds of artificial solids with extremely narrow band structures and, if necessary, combined as optoelectronic devices. This field of research is entitled *Single Electron Logic* (*SEL*) [43], targeting the ultimate miniaturization with electrons.

Initial works for the Single Electron Logic (SEL) and the design of multi-junction devices with chemically-tailored quantum dots

In the meantime, outlines for definitive work and interdisciplinary research projects have matured, whose goal it is to determine the fundamental principles necessary for the design of simple and complex single electron devices based on chemically-tailored quantum dots. Considering the physical and colloid chemical properties of ligand-stabilized clusters in defined three- to one-dimensional organized structures, initial works for nanoscale switches, single electron tunneling transistors, and multi-junction devices should be performed. The main difficulty in using quantum dots in the microelectronics is the simultaneous interconnection and isolation of the dots to allow single electron tunneling between clusters controlled by external voltage sources. In three-dimensional arrangements of ligand-stabilized clusters, this problem is solved in an ideal

way: during pressing to a nearly perfect sphere packing or during crystallization, the ligand shells prevent the clusters from coalescence, acting at the same time as a lubricant and as a "glue". In contrast, the preparation of one- or two-dimensional cluster arrangements requires the development of some new techniques. Depending on the special requirements needed, suitable ligand-stabilized clusters need to be synthesized and modified. Furthermore their special, still unknown electronic and optical properties need to be systematically investigated through suitable microscopic and macroscopic techniques.

In crystals as well as in compressed pellets, the cluster molecules arrange themselves following the principles of closest packing. The "tunneling distance" for charge carriers is the barrier determined by the thickness and chemical nature of the ligand shell. Recent investigations [14, 15] on the "normal" Au_{55} cluster disclose that the energy barrier between the cluster cores in a *three-dimensional arrangement* is still not high enough and the tunnel resistance R_T is not much larger than the quantum resistance R_Q at room temperature. In essence, single charges cannot be localized or stored in or at the single clusters. Excited electrons belong instead to extended states delocalized over wide ranges of the whole solid. Besides using more bulky ligand shells, alternative strategies to increase the barrier level between clusters exist. For example, three-dimensional networks of clusters could be prepared by using chain-like groups as "molecular spacers" (Fig. 14) whereby their functional terminal groups would connect to the cluster and/or the ligand shell via covalent bonds [44].

By adjusting the length of the "spacer" chain, i.e., the number of carbon atoms between the terminal groups, the distance between clusters can be adjusted.

The preparation of *two-dimensional arrangements* like mono- and multilayers of metal clusters can be realized by *self-assembly techniques* or *electro-chemical deposition*: From reports on colloidal chemistry [45] it is known that long chain molecules with terminal sulfone groups attach themselves to the nitrogen atoms of polyethylene-imine layers and arrange themselves as monolayers like Langmuir–Blodgett-Films. Applying this principle to clusters like Au_{55} and Pt_{309} with suitable functionalized ligands, these quantum dots should then arrange on polyethyleneimine films in a similar manner. Another possibility for the two-dimensional self-organization of cluster molecules could be the use of thiolate-ligands [44]. Here, the preferred interaction between sulfur and gold substrate can be exploited to attach sulfur containing ligands to a gold surface. Here, the main requirement for preparing extended colloid or cluster layers is the availability of suitable substrate materials and supports which should lead to an ordered layer growth. A further method is the controlled preparation of metal surfaces with a selected orientation and, if necessary, with small displacements is the cutting of single crystals.

Attempts have been initiated to deposit cluster monolayers electrochemically on electrically conducting substrates like silicon crystals, gold *h*ighly *o*riented *p*yrolytic *g*raphite (HOPG) [46] or glassy carbon. Here, a solution of the sulfonated cluster material in methanol is used for the deposition experiments and the counter electrode is specific for ions in the ligand shell, e.g., sodium or potassium. In this procedure it is important that a redox reaction does not take place, because this would lead to an electrochemical decomposition of the cluster itself.

For the preparation of *one-dimensional arrangements* like quantum wires it is also essential to prepare suitable substrates. Towards this purpose drains having the dimension of a cluster diameter can be etched into selected supporting substrates, to allow a one-dimensional arrangement by adsorption due to the enhanced surface activity (Fig. 15). The technique to prepare these drains is already well-known [47].

Concerning investigations of multi-dimensional cluster arrangements described above, here only those non-optical methods will be emphasized which yielded results pertinent to the SE applications. In this context, one should keep in mind that knowledge about the "function" of cluster systems on the microscopic and macroscopic level is of major importance, but is not a final theoretical explanation of any property. The most useful investigation methods include *Impedance Spectroscopy* as well as the different variants of *Tunneling Microscopy and Spectro-*

Fig. 14 Ligand-stabilized metal clusters chemically linked by a "spacer" molecule

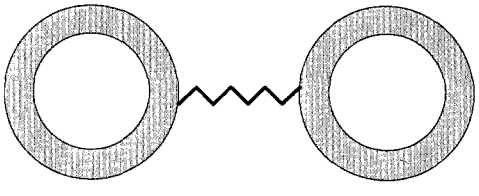

Fig. 15 Top view of a one dimensional arrangement of clusters deposited in an etched drain onto a suitable substrate

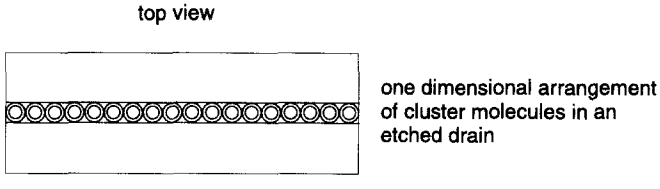

Colloid & Polymer Science, Vol. 273, No. 3 (1995)

scopy for measurements at liquid helium temperature up to room temperature.

As demonstrated in section 6.1 of part I, and section 2.2 of the present work, *Impedance Spectroscopy (IS)* is a macroscopic technique useful for two- and three-dimensional arrangements. From the results of impedance measurements performed on macroscopic samples it is possible to lead the macroscopic properties back to their origin, i.e., the features of single quantum dots at the microscopic scale. As shown, this method allows, via the determination of the time constants and dynamic conductivity, the evaluation of the kinetics of electron transitions between pairs of clusters from the macroscopic relaxation times of collectives of clusters. From temperature-dependent measurements, the activation enthalpy of the single electron transport between clusters (e.g., the Coulomb energy or the disproportionation energy for the inter-cluster process), as well as the influence of the temperature on the DOS of the participating states and, thus on the intracluster electron transport can be determined.

These spectroscopic studies should be supported by techniques which yield structural and morphological information concerning the systems in question. Microscopic techniques for this purpose are *Scanning Tunneling Microscopy (STM) and Scanning Tunneling Spectroscopy (STS)* (see sections 2.1 and 2.3). These techniques allow structural investigations of smallest cluster arrangements as well as the determination of characteristic values for electron transport like I-U-curves, Coulomb barriers, density of states (DOS) in clusters, discreteness of electron states (e.g. level splitting), and the work function [48]. Such data allow the description of the underlying mechanisms for the electron transport. *Atomic Force Microscopy (AFM)* is applied to determine the micromorphology of specially prepared substrates as well as to characterize deposited cluster structures.

Measuring arrangements for the characterization of chemically-tailored systems

A principle common to all measuring arrangements is that the ligand shell which stabilizes the cluster acts, hopefully, as a stable Coulomb barrier to the substrate or a neighboring cluster, while a second barrier is formed by the space (including the ligand shell) between the metal core and the STM-tip or other electrical junction. Measuring pellets of highly condensed cluster material, the rest cluster plays the role of the substrate. This has the disadvantage that the dc-resistance of the whole system becomes extremely high at low temperatures making the observed curves very smeared (c.f. section 2.3).

Some examples of measuring arrangements are outlined which should be investigated by the methods mentioned above. These arrangements should allow addressing and measurements on multi-junctions, although arranged sometimes only by chance:

Three-dimensional samples crystallized or in densest packing, sputtered or unsputtered to plate contact and grids of lines in the scale of a few μm are shown in Fig. 16.

Two-dimensional mono- or multi-layers on conducting or insulating substrates can be addressed as well by sputtered contacts or grids or by a STM-tip (Fig. 17).

One-dimensional systems, like quantum wires, prepared by the deposition of clusters and cluster aggregates in nanosize drains can be addressed by a STM-tip with terminal macroscopic contacts (Fig. 18).

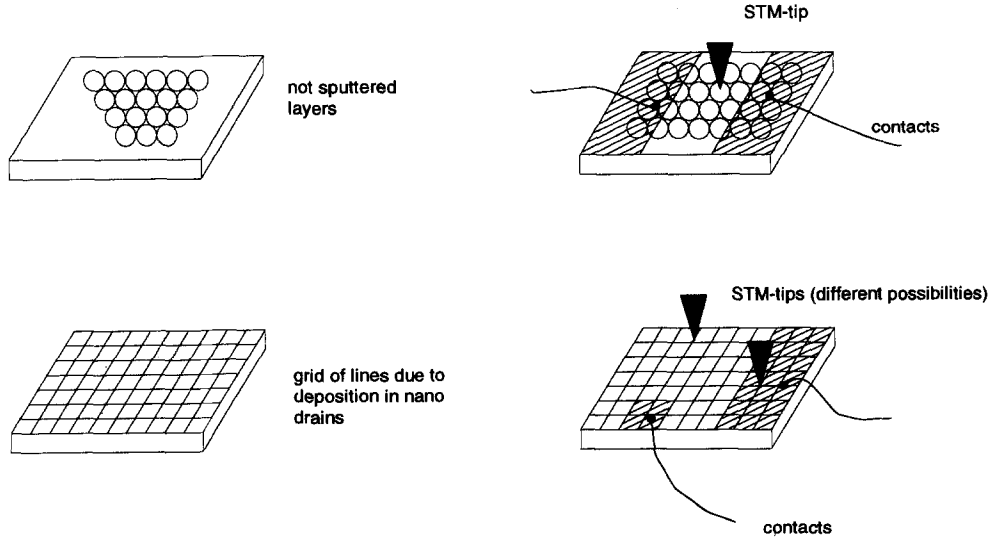

Fig. 16 Different contact and Scanning Tunnel Microscope (STM)-tip arrangements for the measurement of three-dimensional condensed cluster samples

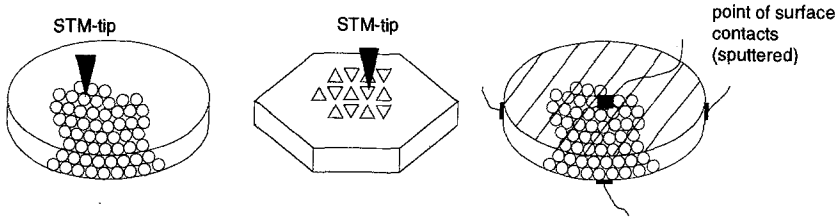

Fig. 17 Various two-dimensional arrangements of quantum dots in layers or deposited in etched linear grids revealing different contact and STM-tip measuring possibilities

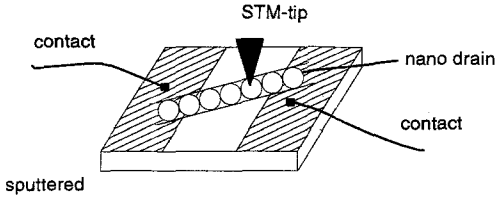

Fig. 18 Contacting of quantum wires constructed from clusters in nano-sized channels

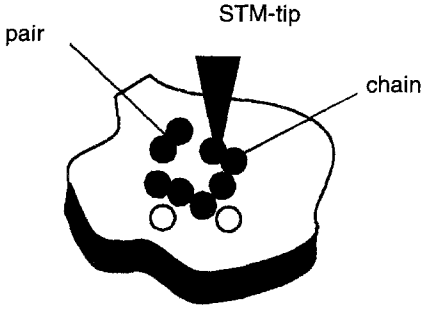

Fig. 19 Deposition of low dimensional cluster arrangements on a suitable substrate using the STM-tip as a "lifting" tool

Zero-dimensional systems: it seems possible to design arrangements of single clusters by using the STM as a "lifting" tool. Here, direct manipulation of clusters to build pairs or chains can be realized (Fig. 19). However, systems containing a large number of clusters could hardly be erected using such a technique.

Applications and perspectives

It is not the purpose of this paper, whose aim is, in fact, to describe a new field in colloid chemistry, to detail concrete microelectronic devices. This would exceed the knowledge of the authors, and here the readers attention should be drawn to other reviews [37, 49–51]. But it should be pointed out that most suggestions deal with much larger devices based on semiconductor materials, even though in the last 10 years, a general understanding of the fundamental principles of conventional SET junctions between metal has been developed by extensive theoretical and experimental work. Conventional SET junctions show the SET effect only at temperatures near the absolute zero and are much larger than single clusters which show the SET at room temperature. One forecast can be made for a possible transition to the *Cluster Single Electronics*: It promises incredibly high density of elements on a chip. Thus, assuming to need the place of say 10×10 clusters for every reliable gate, then for a two-dimensional chip architecture the number of gates might be about 10^{11} per cm^2!

One example for a SE-device working at room temperature may be the "*smallest switch with electrons*" (Fig. 20) [8, 9].

Such a switch consists of two Au_{55} clusters where the ligand shells keep the cluster cores at a distance of 0.7 nm, a barrier easily passed by tunneling. The electrical capacitance of this junction determines the switching offset as well as the temperature at which this quantum device can be used. Regarding this, it becomes clear that the

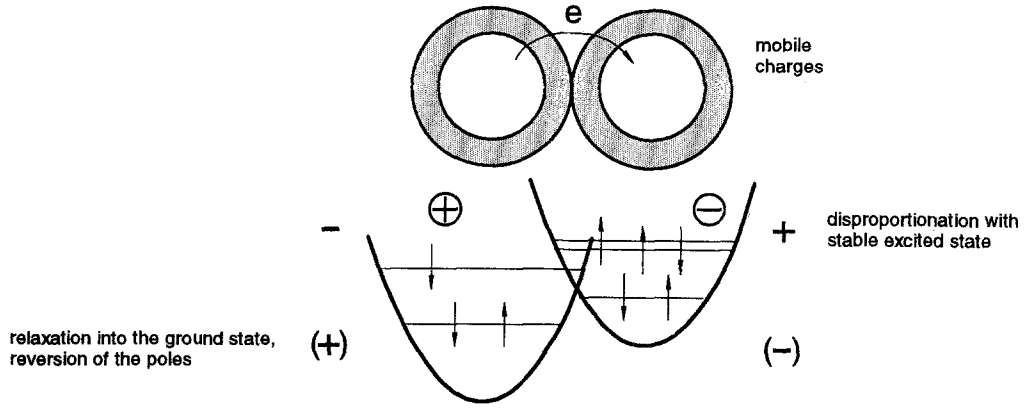

Fig. 20 The "smallest digital switch for electrons" consists of one single cluster pair. Via the transition of one electron by Single Electron Tunneling (SET), this arrangement switches into a disproportionated state

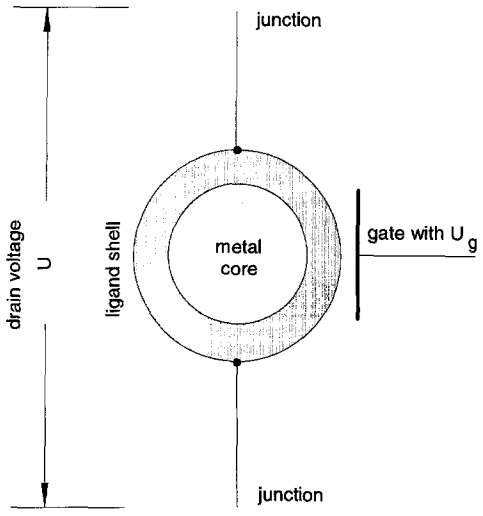

Fig. 21 The "SET transistor" with of metal clusters consists of one single quantum dot with two junctions and one gate electrode

fundamental principle of SET can be directly transfered into a digital technology: Here the binary information is expressed by the absence or presence of one electron (at a special time and a special place) in a quantum dot.

The most detailed concrete ideas involve the utilization of the SET effect in a so-called *SET-transistor* (Fig. 21). This simplest circuit reveals the peculiarities of SE since it includes the usual three junctions but only *one metallic particle*: Two leads must be attached to the particle and this geometry presents the double junction system. The third so-called gate electrode is coupled capacitively for voltage control to the metal island. The sequential transfer of single electrons (or not) depends on the voltage U, applied to the drain electrodes, as well as on the voltage U_g applied to the gate.

Following the suggestions of a growing number of researchers, the SET transistor could be more easily realized and a order of magnitude smaller using chemically-tailored quantum dots like ligand-stabilized quantum dots. This transistor can be used for

- digital circuits and
- highly sensitive electrometers.

The concept of a turnstile (section 2.4) could be used in a single electron pump device with clusters. This is a two-island circuit with three junctions which can be supplied by two, say, sinusoidal signals applied via two gates to both islands. This pump can operate at zero drain voltage U. By a phase difference of 90° it is possible to realize the condition that during one cycle exactly one electron sequentially tunnels through both clusters from one drain to the other. The time constant $R_T C_{\text{micro}}$ for a Pt_{309}-cluster with $R_T \approx 200\ M\Omega$ and $C_{\text{micro}} \approx 5 \cdot 10^{-19}$ F according to formula (1), part I, would then be $\approx 10^{-10}$ s. Such pumping of individual electrons resembles pumping of a liquid across a height difference. This frequency-controlled single electron tunneling opens a possibility to maintain a dc-current I according to the fundamental relationship (2), part I. This is of major importance for the modern quantum metrology to create a

- current standard using with the elementary charge e only one universal constant.

Further applications of ligand-stabilized clusters could be:

- high-frequency devices and
- cellular automata, when $R_T \gg R_Q$.

The field of application could be extended by utilizing the collective properties of chemically-tailored quantum dots, e.g., in

- devices with compact or matrix diluted cluster arrangements including a diluted electron gas which show switchable transparency [9],
- in the photovoltaics in highly efficient thin film photocells where cluster layers replace the conventional semiconductor layers [9],
- in quantum lasers [52], or
- in the nonlinear optics [53].

Out look according to parts I and II of this work

According to the present state of knowledge, colloidal metal particles, like ligand-stabilized metal clusters, in the size range of 1–2 nm are certainly quantum dots. The QSE at the frontier of the transitional state from metallic to molecular structure leads to the localization of some of the last metallic electrons in a quantum box of the lateral dimension of the cluster. The electrons seem to exist in this natural box independent of the unique nature of each respective cluster. These materials present for future microelectronics promising and most fascinating applications in SE. But their exploration requires great interdisciplinary efforts, and time will show how these at present partly speculative forecasts will exactly develop.

With respect to miniaturization employing clusters, currently within reach, we estimated in the preceeding section the enormously high density of gates of 10^{11} per cm^2. An extension of such a novel structure into the third dimension could even amount to a number of gates between 10^{16} and 10^{17} per cm^3. These estimates are actually rather low and based on traditional ideas of information processing. In fact, for cluster networks on molecular scale, the locally interconnected architecture like that mentioned before with cellular automata as

a neural network, seems to be more than adequate for logic and memory cells. But its design and operation principle is presently still rather unexplored.

Particular conditions arise when clusters are organized in novel condensed phases composed of these quantum dots. Within these solids made up of quantum wells with discrete energy levels, the colloidal building elements partly retain their individuality, even when a band-like structure with a transition resistance $R_T \approx R_Q$ is developed in the collective. In the solid, the classical SET-effect, as described by elementary electrostatics, coexists with quantum effects as well. In any case, the relatively simple theory of tunneling across a tunnel barrier, already successfully applied to larger metal particles, may be applied with caution and should certainly be revised for clusters between 1–2 nm. In particular, the standard diffusive single electron transport could be converted into resonant tunneling and ballistic transport [49].

Furthermore, it has also been pointed out that the SET-relations are also valid for superconductivity [37]. An application of this reflection is not so unrealistic, because ideas exist to prepare superconducting devices with high transition temperatures, not only from "pure" clusters, but also from larger doped cluster arrangements similar to the procedure with C_{60}-"crystals" [54] or from clusters with mixed metal-shells [12]. Additionally, it could be advantageous to use defined mixtures of different cluster and ligand shell sizes and materials. Such compact or matrix-diluted devices could also possess "giant magnetoresistance" properties [44].

With the occurrence of the collective phenomena at the coupling of energy quantized electrons in QSET, and the question of what is the influence of energy quantization on SE effects, we enter a fundamental field of quantum physics about which theoretical physicists have just started to think [49, 51]. Monodisperse systems like ligand-stabilized metal clusters have just recently commanded their attention because, at first, these compounds were *not* believed to be in competition with semiconductors. In such structures the electron will behave – as shown here – simultanously as a wave and as a particle. Furthermore, theorists believe that the correlated transmission of electrons does not even require the tunnel effect [49]. One could imagine that there exist still undiscovered three-dimensional solids, "channel" structures with domains of phase coherence for a quasi one-dimensional Peierls-conduction [55], in which, similar to the "tunnel paths" in the brick layer model, the electrons "flow" only in one dimension.

In conclusion, we offer an English translation from the original German of Ligarev and Claeson [49]:
"We believe ... that (the discovery of SE) achieved a contribution to that which could be entitled the psychology of physics. The discovery of correlated tunneling is an example of the fact that an intellectually simple and basic effect remained undiscovered until the mid-1980s. This proves that "Newton's ocean of undiscovered truths" is still full and lies waiting for those scientists – who are equipped with nothing more than their imagination and creativity – to discover them. All those who agree with a theoretical overloading of science and to a billion consuming experiments should think about this."

Cluster-chemistry together with solid state chemistry and again the colloid science belong to the "cheaper" fields of research which may contribute much to the future.

Acknowledgements We thank G. Schmid for cluster materials, intensive cooperation, stimulating discussions, and the exchange of new ideas. We thank as well U. Hartmann and R. Houbertz for cooperation and unpublished measurements. We had helpful cooperation and many discussions on SET with A. Zorin. We gratefully acknowledge financial support from the Bundesiminister für Forschung und Technologie (BMFT), Bonn, (Projekt Nr.:03C 20058) under the coordination of the Deutsche Gesellschaft für das chemische Apparatewesen und Biotechnologie (DECHEMA), Frankfurt, and thank the latter for helpful discussions on particle-size effects.

References

1. Schön G, Simon U (1995) Prog Colloid Poly Sci (in press)
2. Penzar Z, Ekardt W (1990) Z Phys D 17:69–72
3. Genzken O, Brack M, Chabant E, Meyer J (1992) Ber Bunsenges Phys Chem no 9 96:1217–1220
4. Balian R, Bloch C (1971) Ann Phys (N.Y.) 69:76
5. Ozin GA, Bowes CL, Steele M (1992) Mater Res Soc Symp Ser Macromolecular Host-Guest Inclusion Complexes (in press); Ozin GA (1992) Nanomaterials: Endo- and Exosemiconductors, Adv Chem Ser, A.C.S., Washington D.C.
6. Reed M (1993) Spekt d Wiss 3:52–57
7. Cohen ML (1986) Proc 1st NEC Symp, Hakone and Kawasaki, Japan, p. 2–10
8. Schmid G, Schön G, Simon U (1992) German Patent pending No 42–12220
9. Schmid G, Schön G, Simon U (1992) USA Patent pending No 08/041,239
10. Simon U (1992) PhD Thesis University of Essen, Germany
11. Mielke F, Houbertz R, Hartmann U, Simon U, Schön G, Schmid G (1994) Europhys Lett (in press)
12. Schmid G (1992) Chem Rev 92:1709–1727; Schmid G (ed) (1994), VCH, Weinheim (Germany)
13. Schmid G, Lehnert A, Malm J-O, Bovin J-O (1991) Angew Chem Int Ed Engl 30:852
14. Simon U, Schön G, Schmid G (1993) Angew Chem Int Ed Engl No 2 32:250–254

15. Mielke F, Houbertz R, Hartmann U, Simon U, Schön G, Schmid G (1995) (to be published)
16. Vogel W, Rosner B, Tesche B (1993) J Phys Chem 97:11611–11616
17. Smit HHA, Thiel RC, de Jongh LJ, Schmid G, Klein N (1988) Sol St Com 65:915
18. Fairbanks MC, Benfield RE, Newport RJ, Schmid G (1990) Sol St Comm 74:431
19. Marcus MA, Andrews MP, Zegenhagen J, Bommannavar AS, Montano P (1990) Phys Rev B 42:3312
20. Fenske D (private communication), Diploma Thesis University of Karlsruhe, FRG
21. Macdonald JR (1987) Impedance Spectroscopy, John Wiley & Sons, New York
22. van Dijk T, Burggraaf A (1981) Phys Stat Sol a 63:229–240
23. Schouler JL (1979) PhD Thesis Institut National Polytechnique de Grenoble, France
24. Bauerle JE (1969) J Phys Chem Solids 30:2657–2670
25. Simon U, Schmid G, Schön G (1992) Mat Res Symp Proc Vol 272:167–175
26. Möhrke C (1993) PhD Thesis University of Essen, Germany
27. Schmid G (to be published)
28. Smokers RTM (1992) PhD Thesis University of Nijmegen, The Netherlands
29. Zorin AB (1993) (to be published)
30. Schön G (1994) Spektr d Wiss 4:22–24
31. Kolbert AC, de Groot HJM, van der Putten D, Brom HB, de Jongh LJ, Schmid G, Krautscheid H, Fenske D (1992) submitted to Z Phys D
32. Kreibig U, Fauth K, Granqvist C-G, Schmid G (1990) Z Phys Chem 169:11–28
33. Peschel S (1993) Diploma Thesis University of Essen, FRG
34. Funke K (1991) Ber Bunsenges Phys Chem 9:955–964
35. van Staveren MPJ, Brom HB, de Jongh LJ (1991) Physics Reports 208:1–96
36. Licharev KK, Zorin AB (1985) J Low Temp Phys 59:347
37. Gladun A, Zorin AB (1992) Phys i u Z No 4 23:159–165
38. Ozin GA (1992) Adv Mater No 10 4:612–649
39. Deutscher G, Levy YE, Ryazantzev IA, Dravin VA, Yakimov AI (1986) Europhys Lett 4:577
40. Hartman TE (1986) J Appl Phys No 4 34:943–947
41. Schönenberger C, van Houten H, Donkersloot HC (1992) Europhys Lett 20 (3):249–254
42. Nejoh H, Aono M (1993) Jpn J Appl Phys No 1B 32:532–535
43. Averin DV, Register LF, Licharev KK Hess K (1993) submitted to J Appl Phys
44. Schmid G (1993) (to be published)
45. Chi LF, Johnston RR, Ringsdorf H (1992) Thin Film Solids 210/211:211; (1992) Langmuir 8:1360; Chi LF, Anders M, Fuchs H, Johnston RR, Ringsdorf H (1993) Science 259:213
46. Becker C, Fries Th, Wandelt K, Kreibig U, Schmid G (1991) J Vac Sci Technol B9 2:810–813
47. von Klitzing K, Schmid G (1994) unpublished work
48. Binnig G, Rohrer H, Gerber Ch, Weibel E (1982) Appl Phys Lett 40:178; Chen J (1993) Introduction to Scanning Tunneling Microscopy, Oxford University Press, New York
49. Licharev KK, Claeson T (1992) Spektr d Wiss 8:62–67
50. Koch H, Lübbig H (eds) (1992) Single-Electron Tunneling and Mesoscopic Devices, Springer, Berlin Heidelberg
51. Grabert H (ed) (1991) Z Phys B (Special Issue on Single Charge Tunneling) No 3:85
52. Corcoran E (1992) Spekt d Wiss (Sonderheft 11) 1:76
53. Wang Y, Herron N, Mahler W, Suna A (1989) J Opt Soc Am B Vol 6 No 4:808–813
54. Fink J, Sohmen E (1992) Phys Bl No1 48:11–15
55. Hamann C, Burghardt H, Frauenheim T (1988); Ebeling W, Weißmantel Ch (eds), VEB, Berlin, 101–119